

BLACK HOLES AND WORMHOLES IN 2+1 DIMENSIONS

Stefan Åminneborg^{*1}

Ingemar Bengtsson^{**2}

Dieter Brill^{***3}

Sören Holst^{**4}

Peter Peldán^{**5}

** Norra Reals Gymnasium, S-113 55 Stockholm, Sweden*

*** Fysikum, Stockholm University, Box 6730, S-113 85 Stockholm, Sweden*

**** Department of Physics, University of Maryland, College Park, MD 20742,
USA*

Abstract

A large variety of spacetimes—including the BTZ black holes—can be obtained by identifying points in 2+1 dimensional anti-de Sitter space by means of a discrete group of isometries. We consider all such spacetimes that can be obtained under a restriction to time symmetric initial data and one asymptotic region only. The resulting spacetimes are non-eternal black holes with collapsing wormhole topologies. Our approach is geometrical, and we discuss in detail: The allowed topologies, the shape of the event horizons, topological censorship and trapped curves.

¹Email address: stefan@vanosf.physto.se

²Email address: ingemar@vana.physto.se

³Email address: brill@umdhep.umd.edu

⁴Email address: holst@vanosf.physto.se

⁵Email address: peldan@vanosf.physto.se

I. Introduction.

Black holes in 2+1 dimensions are remarkable and surprising not only by their mere existence, but also because of the wide variety and topologically distinct types of black-hole spacetimes that can be constructed. All of these exist as solutions of the sourcefree Einstein equations only if there is a negative cosmological constant, and hence they are asymptotically anti-de Sitter rather than asymptotically flat. We concentrate attention on such spacetimes that have just one asymptotic region, but a complex interior topology.

In 3+1 dimensions the simplest (Schwarzschild-Kruskal) black hole has two asymptotic regions, and is eternal in the sense that a horizon for each asymptotic region exists for all times. Black holes with one asymptotic region are typically the result of gravitational collapse (of gravitational waves in the source-free case), and are therefore not eternal. There are also more bizarre black hole spacetimes that have only one asymptotic region, with a horizon that starts at some time somewhere in the interior, but in which there is no collapse of waves from the exterior. An example is the “RP³” geon [1], a non-orientable quotient space of the Schwarzschild spacetime. The details of the dynamics of non-eternal black holes can be rather difficult to analyze; much of what we know about their horizons and how it starts comes from numerical work.

By contrast, in 2+1 dimensions all the details of the black hole solutions can be analyzed exactly. This is of course due to the absence of local gravitational degrees of freedom (gravitational waves); but global and topological degrees of freedom still exist in 2+1 dimensions—in particular we will see that there is an analog of the black holes with wormhole topology. Thus, in 2+1 dimensions a great variety of simple models allow detailed investigation, for example of the collapse and of the horizon.

In this paper we show the construction of 2+1 dimensional black holes with a single asymptotic region and arbitrary spatial topology in the interior. By spatial topology we mean the 2-dimensional topology of spacelike surfaces Σ that foliate the spacetime. (They are not Cauchy surfaces since the spacetime is modeled on anti-de Sitter space, which is not globally hyperbolic.) The topology of such 2-dimensional surfaces is classified by genus and orientability, and we will see that all topologies with genus ≥ 1 are allowed. We will give a complete account of trapped surfaces and the shape of the event horizon for the simplest wormhole topology, and indicate what the situation is for the more complicated cases.

In section II we recall the essential features of a single (non-rotating) 2+1 dimensional black hole, the “BTZ black hole.” In section III we introduce a particular point of view [2, 3] which enables us to construct a variety of such black holes. Section IV introduces simple “building blocks”, out of which black holes of all interior topologies can be constructed. Section V discusses the spacetimes that result, with particular attention to the exterior and to the event horizon. Section VI is devoted to topological censorship. Section VII focuses on

the trapped surfaces and apparent horizons of these spacetimes. Two appendices describe the coordinate systems that we use to visualize the constructions.

II. The Geometry of the Simplest Black Hole Solution.

The 2+1 dimensional black hole found by Bañados, Teitelboim and Zanelli [4] is easily described in terms of Schwarzschild-like coordinates,

$$ds_{BTZ}^2 = - \left(-M + (r/\ell)^2 \right) dt^2 + \frac{dr^2}{\left(-M + (r/\ell)^2 \right)} + r^2 d\phi^2 . \quad (1)$$

(Here we have confined attention to the case without angular momentum, because spinning black holes are difficult to handle with the methods that we will use.) To cover the complete spacetime we need to allow r to vary between 0 and ∞ , with the usual Kruskal-type analytic extension across the lightcone $r = M$. The coordinate ϕ is understood to have periodicity 2π ; if it instead is allowed to range over all of \mathbb{R} , the metric describes (a part of) anti-de Sitter (adS) space. To understand the resulting global geometries more directly, other representations are useful.

Since all known 2+1-dimensional black hole geometries are quotient spaces of adS space under a group of isometries, we first consider a representation of adS space itself. We introduce a flat 4-dimensional space with a metric of somewhat unusual signature,

$$ds^2 = -dT^2 - dU^2 + dX^2 + dY^2 . \quad (2)$$

Then the 2+1-dimensional adS space can be embedded in this flat space as the hyperboloidal surface

$$-T^2 - U^2 + X^2 + Y^2 = -\ell^2 . \quad (3)$$

(We will set the scale factor $\ell^2 = 1$ from now on.) This surface is periodic in time, so true adS space would be the covering space of this surface. This distinction is however immaterial for the black holes, which involve less than one period of the surface. Indeed the covering space of our black hole spacetimes is a proper subset of the hyperboloid.

One way to describe 2+1-dimensional black holes is to specify the isometry group by which points in adS space are to be identified. Alternatively we can choose a fundamental region of the isometry and describe the spacetime by the identifications of the region's boundaries implied by the isometry. The isometries are the rigid motions $SO(2,2)$ that leave the origin of the embedding space fixed and its metric invariant. These isometries map adS space (3) into itself.

The discrete group of transformations corresponding to a BTZ black hole is generated, for example, by the ‘‘Lorentz-type’’ adS transformation

$$T' = T \cosh(2\pi\sqrt{M}) + Y \sinh(2\pi\sqrt{M}) \quad U' = U \quad (4)$$

$$Y' = T \sinh(2\pi\sqrt{M}) + Y \cosh(2\pi\sqrt{M}) \quad X' = X.$$

A possible fundamental region is therefore given by the (double) wedge

$$-T \tanh(\pi\sqrt{M}) \leq Y \leq T \tanh(\pi\sqrt{M}) \quad (5)$$

whose boundaries are to be identified according to the transformation (4). The edges of the wedge are the fixed point sets $T = 0$, $Y = 0$; these are considered as singular points in the BTZ geometry. The covering space of the BTZ black hole is then given by a subset of adS space in which the Killing vector $J_{TY} = T\partial_Y + Y\partial_T$ (which generates the discrete isometry) is spacelike.

In addition to BTZ coordinates, there are two other convenient sets of coordinates within adS space called “stereographic” and “sausage” coordinates. The stereographic coordinates express the metric in a form which is manifestly conformally flat, and are therefore very helpful for visualizing lightlike surfaces. The sausage coordinates foliate adS with Poincaré disks and have the advantages that they are static and cover the whole manifold. Sausage coordinates are uniquely defined and make the time-symmetry manifest, whereas stereographic coordinates can be “centered” on various points of the spacetime (antipodal to the center of projection). Both of these coordinate systems have the virtue that they can bring points at infinity to finite coordinate values—they provide us with a kind of 3-dimensional Penrose diagrams.

In this paper we will not use intrinsic coordinates to carry out calculations, but we will frequently draw pictures to visualize our constructions. In these pictures either stereographic or sausage coordinates will be used. For the convenience of the reader all details about the coordinate systems are given in the appendix (they can also be found in previous publications [5] [6]). The resulting pictures of the fundamental region of the BTZ black hole are given in figure 1.

When the fundamental region is given it is easy to identify the event horizon. It is simply the boundary of that part of the fundamental region which cannot be seen from its conformal boundary (\mathcal{S}). Figure 1 shows this construction for the BTZ solution, and we see that this spacetime is a genuine black hole since indeed only a part of the fundamental region can be reached by past directed null geodesics from \mathcal{S} . The fundamental region always has the property that points that are left fixed by some element of the group can occur (if at all) only on its boundary, where they will give rise to “corners” or “folds”. In figure 1b, which covers the entire fundamental region, there are two lines of fixed points, one in the future and one in the past. A fixed point gives rise to a singularity in the quotient space. In spacetimes with Euclidean signature only conical singularities arise in this way, but the singularities of

the BTZ solutions are of a different nature. Indeed, at the cost of admitting closed timelike curves, it is possible to extend the solution analytically beyond these singularities to some extent, to see this, note that the part of the solution which is covered by the stereographic coordinates is conformal to 2+1 dimensional Misner space [7]. By means of stereographic coordinates centered on different points we can cover the entire BTZ black hole with two Misner spaces. The singularity of a Misner space is well understood, and the singularities of the BTZ solution have the same properties. In this paper we simply refer to them as “singularities”, and our only concern is to ensure that they are hidden behind an event horizon (unless they occur at the beginning of the universe).

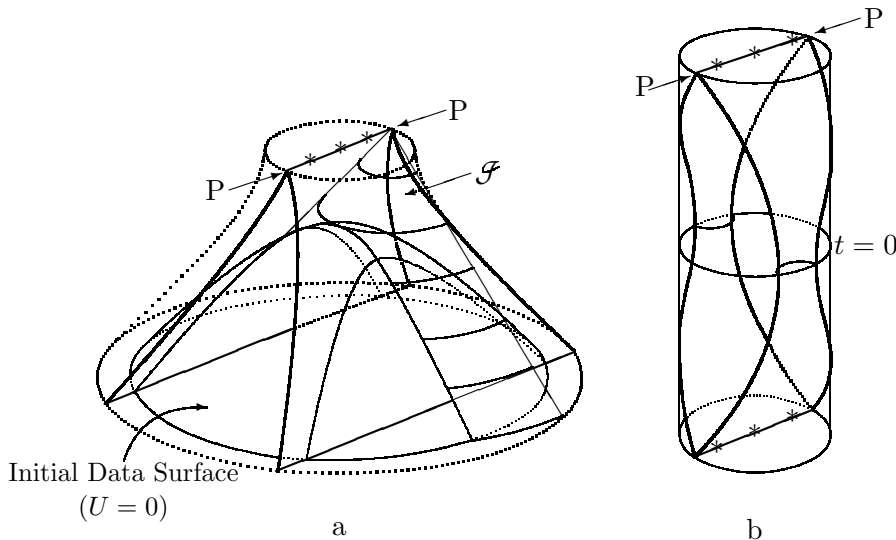


Fig. 1: The fundamental region of the BTZ black hole within adS space, indicated by the heavy outline. The left and right boundaries of this region are to be identified. The identification generates two lines of singularities as indicated by “barbed wire” lines, containing crosses. The singularity meets infinity at points such as those denoted by P. (a) Stereographic coordinates centered on the future singularity cover only somewhat more than half of the fundamental region. The complementary patch, covering the past singularity, would be a mirror image of this figure about a horizontal plane. Infinity is represented by the dotted hyperboloid. The event horizon of one of the two parts of null infinity is given by the backwards light cone (horizontal stripes) from the end point P of that null infinity (\mathcal{F}).

(b) In sausage coordinates infinity is represented by a cylinder. These coordinates cover all of the fundamental region, and the symmetry about the initial data surface $t = 0$ is manifest. The same surface occurs as the $U = 0$ hyperboloid in the figure on the left.

III. Constructing Black Holes from Initial Data.

How can we generalize the BTZ solution? Let us for the moment set aside the spacetime properties of our black holes, and instead adopt an initial value point of view [2][3]. Since adS space is not globally hyperbolic the future of a set of initial values is not determined by Cauchy data alone, but this does not prevent us from singling out a moment in time and studying the spatial geometry at that moment. Specifically, let us choose the spatial surface defined by

$$U = 0 \quad -T^2 + X^2 + Y^2 = -1 \quad T > 0 . \quad (6)$$

This is one sheet of a two dimensional hyperboloid embedded in the flat 3-dimensional Minkowski space that is defined by $U = 0$. (As such it would seem to have non-vanishing extrinsic curvature; but note that as a subspace of the 3-dimensional surface (3) its extrinsic curvature vanishes!). It is well known⁶ that the intrinsic geometry on such a surface is a model for Lobachevsky’s hyperbolic geometry H^2 , and that it is equivalent (under stereographic projection) to that of the Poincaré disk. On the latter, spatial geodesics are represented by circular arcs that are orthogonal to the boundary of the unit disk; angles are represented accurately in such a picture, while distances are distorted. Because the extrinsic curvature of the surface (6) vanishes, the isometry which gave rise to the BTZ black hole is also an isometry of our spatial slice; indeed it acts like a hyperbolic Möbius transformation—which we will call a “transvection”.

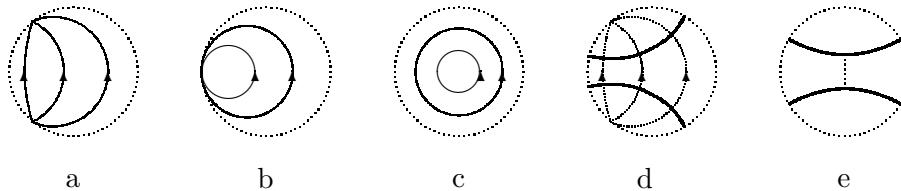


Fig. 2: Isometries (a-c) and fundamental regions (d,e) of the Poincaré disk. Continuous isometries are shown by their flow lines. Discrete isometries are defined by their fundamental regions in heavy outline. Infinity is the dotted boundary of the disk. The isometries are (a) a transvection (with two fixed points on the boundary of the disk), (b) a parabolic Möbius transformation (with one fixed point on the boundary) and (c) a rotation (with one fixed point in the interior, in this case at the center of the disk). (d) A fundamental region of a BTZ black hole at the moment of time symmetry, obtained by identification under a discrete version of the isometry shown in (a). (e) The same fundamental region as in (d), after applying a transvection to move the event horizon (dotted line) to the center of the disk; like the boundaries of the fundamental region, the event horizon at the moment of time symmetry is a geodesic.

⁶For details see, for example, reference [8].

Figure 2 is intended to remind the reader about the flow of the various kinds of isometries that act on the Poincaré disk. An interesting fact is that there is one and only one flow line of a transvection which is also a geodesic. The figure also shows the intersection of the fundamental region of the BTZ black hole with the disk; its boundaries are two geodesics. It is easy to locate the intersection of the event horizon with the disk, since it is in fact the intersection of two totally geodesic surfaces, and hence a geodesic on the disk. Since it is also closed, it must coincide with the unique geodesic flow line of the identifying transvection.

This construction suggests some obvious generalizations. For example, we can use a parabolic Möbius transformation to carry out the identification. This gives us a “ $M = 0$ ” (extremal) BTZ black hole (Fig. 3a). Or we can use a group generated by more than one transvection. As is well known [8], such groups can be defined by assigning a polygon with $4g$ geodesic sides as a fundamental region and arranging the identifications so that all corners are identified as one point. As long as we arrange for the sum of the polygon’s angles to equal 2π the result is a smooth compact Riemann surface of genus g (fig. 3b). In this way we obtain Riemann surfaces of constant negative curvature for any genus $g \geq 2$; the case of genus one is excluded since the sum of the angles of a hyperbolic square is necessarily less than 2π , which means that the resulting torus will have a conical singularity. In the literature on 2+1 gravity [9] conical singularities are often taken as models of point particles, but in this paper we adopt the convention that no singularities are admitted, unless they are hidden by event horizons. Having decided this we have to face the fact that the torus does not admit a metric of constant negative curvature. We can avoid this problem by poking a hole in the torus, and throwing the boundary of the hole to infinity. The fundamental region of Figure 3c (with geodesic sides identified crosswise) indeed gives rise to a smooth non-compact quotient space of this kind.

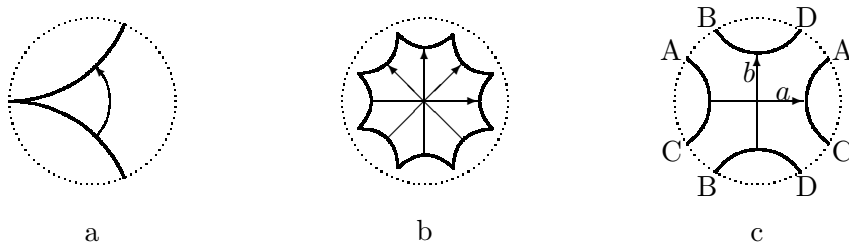


Fig. 3: Initial data represented by fundamental regions and identifications (arrows), corresponding to (a) an extremal black hole, (b) a compact universe of genus 2, and (c) a wormhole with one asymptotic region. The latter has only one asymptotic region since the path $A \rightarrow B \rightarrow C \rightarrow D \rightarrow A$ is closed.

To evolve these data in time, we note that the extrinsic curvature tensor vanishes, so we have a time symmetric initial value problem; but since adS

space is not globally hyperbolic, further information is needed to specify the spacetime. We bypass this problem by adopting the rule that the spacetime is given by extending the action of the discrete isometry group to anti-de Sitter space, and then we construct the quotient space. This is of course equivalent to extending analytically beyond the initial data's domain of dependence. When this procedure is applied to the initial data in Figure 2d we recover the BTZ black hole. For the initial data in Figure 3 we obtain respectively an extremal black hole [4], a compact universe which begins and ends with a singularity [10] [5], and a new kind of 2+1 black hole that is the subject of this paper.

It may be useful to restate our strategy in spacetime terms as follows: We are interested in spacetimes that can be obtained from anti-de Sitter space as the quotient space adS/Γ , where Γ is a discrete group which acts properly discontinuously on some subset of adS . Such spacetimes were given a thorough treatment by Mess [10], who classified all the quotient spacetimes that can be obtained in this way and which have the topology $\mathbf{S} \otimes \mathbb{R}$, where \mathbf{S} is a closed spatial surface. For our purposes this is not enough. We want non-compact spaces (so that infinity can be defined), and we admit groups with fixed points, but only if the corresponding singularities in the quotient space are hidden behind event horizons. To identify such black hole solutions we need to understand the causal structure of the entire quotient spacetime. For this reason we restrict our problem by the demand that Γ shall transform the surface $U = 0$ into itself, which means that Γ belongs to a diagonal $SO(2, 1)$ subgroup of $SO(2, 2)$. As we will see this is enough to make our problem manageable. (The restriction is clearly severe, in particular it excludes the spinning black hole found by Bañados, Henneaux, Teitelboim and Zanelli [4]. We will comment briefly on this point in the concluding section.) Even so discrete groups of this kind are notoriously difficult to describe by their Lorentz matrix representation. The most practical way to define a particular discrete group is to specify a fundamental region on the initial Poincaré disk, $U = 0$. The properties of adS/Γ can then be found through an analysis of the fundamental region in adS . For example, in Fig. 3c Γ is the discrete group that is generated by the two transformations a and b that identify opposite sides. A similar prescription may be adopted for Fig. 3b, but in the latter case the generators are subject to a restriction which ensures that the sum of the angles of the octagon is 2π .

Let us give a brief sketch of our new black hole here (to be followed by a careful analysis in sections V-VII). The fundamental region in Fig. 3c serves to define the two group elements a, b that generate Γ . It is then straightforward to find the fundamental region in anti-de Sitter space; we draw its spacetime portrait in sausage coordinates in Fig. 4. It looks like a tent with four openings and totally geodesic sides that meet at four “folds” in the roof of the tent. The folds are lines of fixed points for certain elements of Γ . To see this it must be remembered that Γ has an infinite number of elements even though it has only two generators. The general element transforms a fold into another fold that may lie in another image of the fundamental region, outside the tent; but

there are particular elements, of the type $aba^{-1}b^{-1}$ that leave a particular fold fixed. These elements give rise to singularities in the quotient space. Drawing the picture is a quick way to locate these lines. It should be kept in mind that in the quotient space, that is after the identifications according to a and b have been made, there is really only one asymptotic region, and similarly there is only one fold in the roof.

In analogy to the case of the BTZ black hole, it is evident that all of the interior of the fundamental region cannot be seen using null lines from the openings of the “tent”. By definition, the hidden region is the black hole. Since the folds in the roof cannot be seen from the openings the resulting singularities are hidden inside the black hole—no naked singularities will be created.

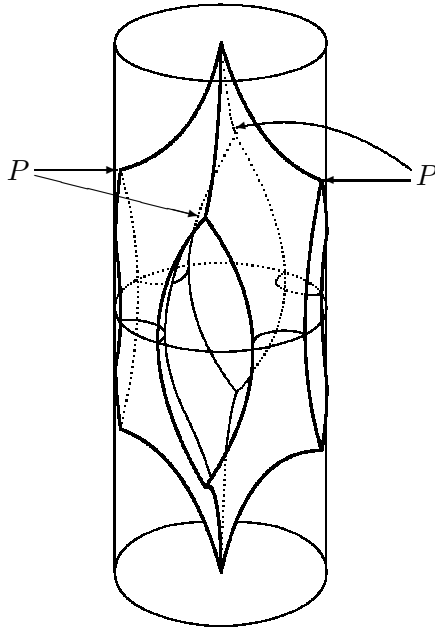


Fig. 4: The fundamental region of the new black hole. The points labelled by P are really the same point, and the event horizon is the backwards light cone of this point. (In stereographic coordinates centered on the time-symmetric surface the topology of this figure would be the same, but all surfaces, including the limiting cylinder, would become hyperboloids. For a stereographic cross section see Fig. 10.)

IV. Spatial Topology.

In this section we discuss the various topologies that occur as solutions of Einstein’s equations with a negative cosmological constant, and find their global degrees of freedom. We confine attention to time-symmetric geometries with a

single asymptotically de Sitter region. The extension of the analysis to cases with several asymptotic regions is quite straightforward.

We will consider the initial geometry on a surface of time symmetry. The only condition on this 2-dimensional spacelike geometry is the Einstein constraint, which in the case under consideration (time symmetry means vanishing extrinsic curvature) demands that the intrinsic geometry have constant curvature. If space is closed this means that all topologies with genus $g > 1$ are admitted, and no others. But we will consider the non-compact case.

We have found two ways of constructing such 2-dimensional spaces S useful. We made use of the first already in section III, where the initial data slice appeared as the quotient by a suitable group of isometries⁷ of the universal cover, the simply connected space H^2 of constant negative curvature, conveniently represented as the Poincaré disk.

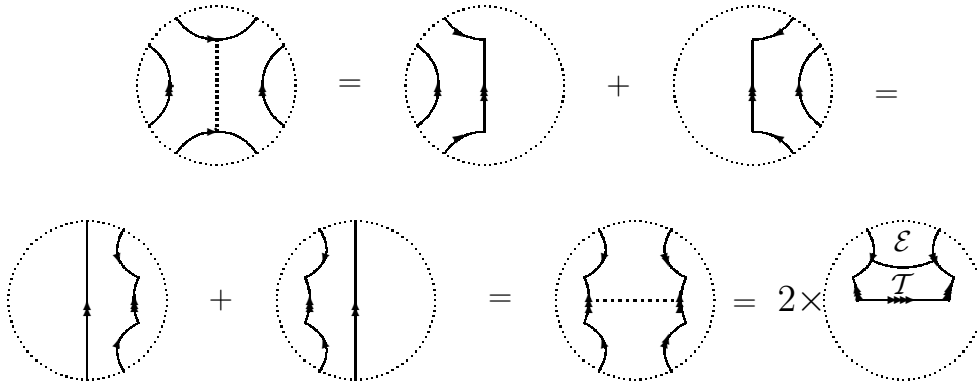


Fig. 5: Different but equivalent ways to construct initial data of a black hole of the wormhole type. We begin with a fundamental region of the kind that was used in the previous section, having one asymptotic region only (although this is not immediately apparent from the picture). Then we cut the disk in two, apply a global isometry to the two pieces, and glue them back together in a new way. Finally we cut the new disk in two to obtain two disks, which we refer to a “doubling” of the initial data. The fundamental region on the new pair of disks naturally splits in two pieces, a hyperbolic hexagon \mathcal{T} representing the interior of the black hole together with an exterior region denoted \mathcal{E} . Gluing the hyperbolic hexagons together we obtain the “pair of pants” used in Figure 6.

For each such isometry group one can find a fundamental region that yields S when its boundaries are identified according to the isometries. It is always

⁷As remarked before, in this paper we exclude groups with fixed points on the initial surface, which would give rise to particle-like singularities. This is to be contrasted with the spacetime isometry group, where we do want fixed points in order to generate black holes.

possible to choose this region to have geodesic boundaries. The first of the disks shown in Figure 5 illustrates a fundamental region for a black hole with a single exterior and a toroidal interior, which is the type of black hole of primary interest in the following sections. Boundaries bearing an equal number of arrowheads are to be identified with each other. An advantage of this representation is that only a single region is needed; a disadvantage is that for more complicated topologies the identifications are not easy to visualize, nor is it apparent how to count the parameters that specify the geometry (as a matter of fact there are three parameters, the geodesic distance between the boundaries and an additional angle).

The second construction builds S combinatorially out of simple blocks. The boundaries of these building blocks are chosen to be geodesic, so the only smoothness condition (which determines whether two blocks fit together) is that the lengths of the boundaries agree. The blocks can be easily visualized by “doubling” a region bounded by 3 resp. 6 geodesics. The last part of Figure 5 shows such a doubling, where unmatched boundaries are identified between the first and second copy of the figure. (Note that mathematicians use the word “doubling” in a different way [8]). When the pair of disk regions is glued together in this way we obtain a three dimensional picture of the initial data as shown in Figure 6a. A minimal geodesic divides it into a region called “trousers” \mathcal{T} and an exterior region \mathcal{E} .

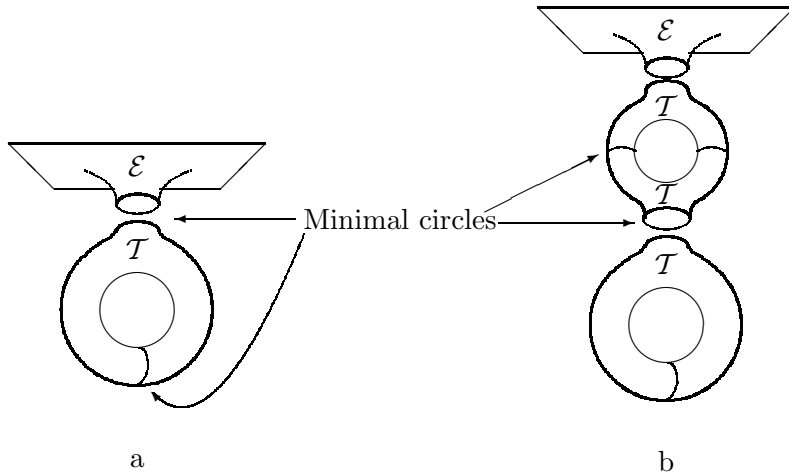


Fig. 6: Construction of the class of spaces considered here by sewing together a set of trousers and one asymptotic region (which looks asymptotically flat in the picture, but which does in fact have constant negative curvature everywhere, just like the trousers).

Regions of these two types can also be glued together to form more complicated topologies (Figure 6b). By an (orientable) 2-surface of genus g with one asymptotic region we mean a topology of the type $\mathbb{R}^2 \# \mathbb{T}^2 \# \dots (g \text{ factors}) \dots \# \mathbb{T}^2$,

that is a plane with g handles attached. For any noncontractible circle in a space of this topology there is a homotopic minimal circle. We can choose $3g - 1$ such circles that divide the surface into an exterior \mathcal{E} and $2g - 1$ trousers \mathcal{T} . Figure 6a shows how this is done for the black hole with a toroidal interior, $\mathbb{R}^2 \# \mathbb{T}^2$, and Figure 6b shows how further handles are inserted.

In this description we can choose as the parameters the horizon length of the exterior, the length around each opening of the trousers, and the amount of twist by which two openings are turned before identification. Thus in Fig 6a the trouser “legs” that are identified have to have the same circumference, and the trouser “waist” must have the same circumference as the exterior horizon, so there are two length parameters. In addition there is one twist parameter at the legs. (The twist at the waist does not change the geometry, because the exterior is rotationally symmetric.) Thus we find 3 parameters determining this geometry, as above. It follows from figure 6b that adding a handle yields 3 more lengths and 3 more twists, so the genus g geometry is characterized by $6g - 3$ parameters. These parameters span a $(6g - 3)$ -dimensional space known as Teichmüller space; it is the space of two-geometries modulo the connected component of the diffeomorphism group and modulo conformal transformations. (This is a well known mathematical construction [8]. In our case the conformal factor is fixed by the requirement of constant curvature. The length and twist parameters are known as Fenchel-Nielsen coordinates on Teichmüller space.)

The moduli space or “superspace” (in the sense of Wheeler and Fischer [11]) of these 2-geometries is also $(6g - 3)$ -dimensional, but due to invariances under “large” diffeomorphisms it has a non-trivial topology. (For example, a twist by 2π leaves the geometry unchanged; two wormholes that “look” different may nevertheless have the same intrinsic geometry.) Thus the superspace of our black hole initial states has its usual structure of a stratified manifold, with the strata representing geometries of greater symmetry; it is more difficult to understand in detail than Teichmüller space.

V. Time Development of the Wormholes.

The simplest wormhole is evidently the toroidal one, so let us focus on this case first. We also choose the fundamental region to be as symmetric as possible, so that the discrete isometry group Γ that it defines is generated by the isometries $a = e^{\gamma J_{TX}}$ and $b = e^{\gamma J_{TY}}$, with the same real number γ in both cases. (That is, we concentrate on a one parameter family of toroidal wormholes, rather than on the three parameter family that we have shown to exist.) Here J_{TX} and J_{TY} are the Killing vectors

$$J_{TX} = X\partial_T + T\partial_X \quad J_{TY} = Y\partial_T + T\partial_Y . \quad (7)$$

They clearly preserve the surface $U = 0$, and we assume that γ is large enough so that an asymptotic region exists. Next we extend the action of the isometries to anti-de Sitter space, and we choose the fundamental region as depicted in

figure 4 above (using sausage coordinates). As noted, the folds in the roof of the “tent” define lines of fixed points of some of the isometries; we pushed the fixed points away from the initial disk by opening an asymptotic region, but with the passage of time they are coming back into our spacetime. However, since the folds cannot be seen from infinity such singularities are allowed. It is also worth observing that our spacetime has no global Killing vector (this is evident since such a Killing vector would have to commute with both J_{TX} and J_{TY} , which is impossible); it may of course still have discrete symmetries.

The event horizon is defined as a surface that bounds a region of spacetime which cannot be seen from \mathcal{F} , which in our picture consists of the openings of the “tent”. It can actually be a little tricky to find the event horizon from a given choice of fundamental region. However, our choice does not belong to the tricky ones, since the identifications are such that they can never cause a curve to turn back in “sausage time” t . It is therefore evident that the event horizon is given by the backwards light cone of the last point on \mathcal{F} (in Figure 4 this appears as four points to be identified, marked P).

For a first study of the exterior of this black hole, let us return to the initial data point of view, and more particularly to the series of cuttings and gluings that turned our original fundamental region into two hyperbolic hexagons. This time we do not glue these together into a pair of pants, but into a single region in the Poincaré disk as in Figure 7. It is now manifest that there is one asymptotic region only; moreover the event horizon is easily located since—as explained in section III—it must be the unique geodesic that is to be found among the flowlines of the transvection that identifies the two external boundaries of the fundamental region.

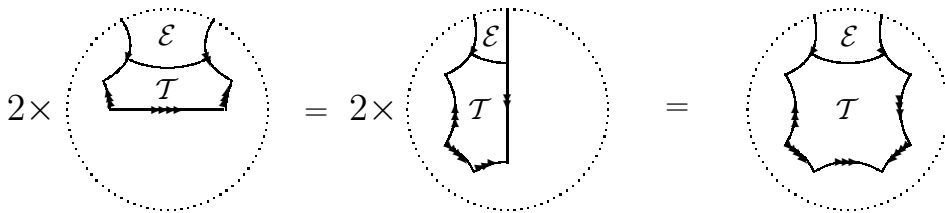


Fig. 7: Making it manifest that our initial data leads to one asymptotic region only. We start with the last frame of Figure 5, apply a global isometry and glue the two parts together. The line dividing the regions \mathcal{E} and \mathcal{T} is the event horizon at the moment of time symmetry.

Now the point is that the region denoted \mathcal{E} is isometric to the exterior of the BTZ initial data. To the future and past of this region there will be a part of the exterior isometric to the exterior of the BTZ black hole. It is a region of spacetime that contains a static Killing vector, and to the future of the moment of time symmetry it is bounded by the event horizon on one side and by \mathcal{F} on the other. We emphasize that this does not mean that our wormhole is

observationally indistinguishable from the BTZ black hole. Indeed the BTZ exterior forms only a subset of the exterior of the wormhole; to the past of the moment of time symmetry the behavior of the event horizon differs drastically between the two cases, as we will see. However, the BTZ exterior agrees with the domain of outer communication of the wormhole, which by definition is the set of points that can be reached from \mathcal{F} by causal curves in both the past and the future direction.

Let us describe the construction analytically, using the embedding coordinates of Eq (3) for this purpose. The fundamental region (depicted in Figure 4) is bounded by the surfaces

$$\frac{X}{T} = \pm \tanh \frac{\gamma}{2} \equiv \pm \alpha \qquad \frac{Y}{T} = \pm \tanh \frac{\gamma}{2} \equiv \pm \alpha . \quad (8)$$

The real number α is as convenient a number as any to parametrize our black hole. We observe that

$$\frac{1}{\sqrt{2}} < \alpha < 1 , \quad (9)$$

and that the length of the event horizon grows with α , so that a large value of the parameter corresponds to a large mass for the black hole. The lower limit on α guarantees that an asymptotic region exists—there is no extremal black hole of this toroidal type that has vanishing mass. The last point on \mathcal{F} occurs when the folds in the roof of the tent reach the boundary of spacetime, which happens for sausage time $t = t_P$ and stereographic time $\tau = \tau_P$, where

$$\tan t_P = \sqrt{2\alpha^2 - 1} = \frac{1}{\tau_P} \qquad \text{hence} \qquad 0 < t_P < \frac{\pi}{4} . \quad (10)$$

Since it takes an amount $\pi/2$ of sausage time for a radial light ray to go from the origin of adS to its boundary, it is evident that the event horizon is born at the time $t_{birth} = t_P - \pi/2 > -\pi/2$. But spacetime itself is born at $t = -\pi/2$, i.e. before the event horizon; this is not an eternal black hole.

At late times the event horizon is the smooth backward light cone from the last point on \mathcal{F} . If such a point is given in stereographic coordinates by (x_P, y_P, τ_P) then the backward light cone is given in stereographic coordinates by

$$(x - x_P)^2 + (y - y_P)^2 - (\tau - \tau_P)^2 = 0 . \quad (11)$$

When we use stereographic coordinates this appears as a null cone with its vertex on the boundary of spacetime similar to fig 1a, but in anti-de Sitter space itself it is really a null plane since its null generators have zero convergence and the vertex is infinitely far away. In embedding coordinates the expression becomes

$$x_P X + y_P Y - \tau_P T - U = 0 . \quad (12)$$

There will actually be four such surfaces in our fundamental region, since the last point on \mathcal{F} appears as four points to be identified. Eventually the surfaces

will intersect, which leads to caustics in the horizon (where new generators are added to it). In order to understand the shape of the horizon we use sausage coordinates and draw a sequence of equal- t slices. To locate the event horizon it is easiest to draw these pictures starting from the moment when \mathcal{F} disappears, and then to follow the evolution backwards in time. The result is displayed in Figure 8; when read from right to left this figure shows how the event horizon moves outward from the point at the spatial origin where it is born.

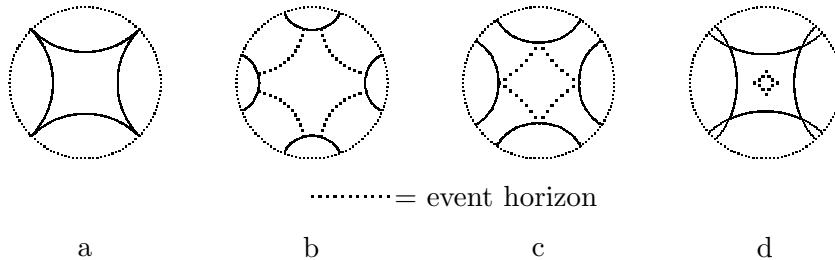


Fig. 8: We follow the event horizon backwards in time. The first slice (a) is at t_P . The next (b) is at $t = 0$, the moment of time symmetry. Then the event horizon is a smooth circle, and it remains smooth until the next earlier slice (c) when the different pieces of the horizon meet each other at the identification surfaces. Before that moment the horizon has four kinks and is growing outward. The final slice (d) shows the geometry just after the event horizon is born as a point at the origin (at a time t_{birth} when the asymptotic region does not exist).

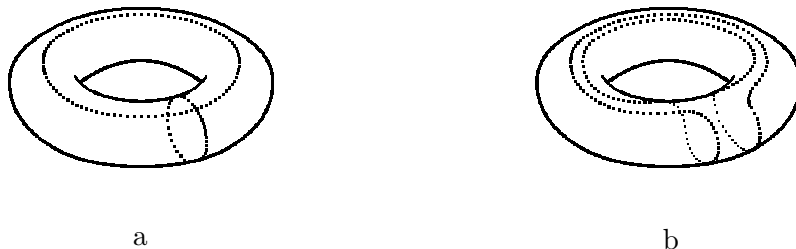


Fig. 9: The event horizon (dotted curves) is born as two intersecting circles on the torus (a). It is possible to find a spatial slicing (b) such that the event horizon becomes a smooth curve a moment after. However, the slice in which the horizon is born cannot be smooth since the caustics have a kink at the point where they intersect. Hence this picture is topologically accurate but metrically misleading.

Note that the kinks in the event horizon are moving outward faster than light; otherwise expressed, the event horizon grows from a pair of spacelike caustics. If we consider slices of equal stereographic time τ instead we find that the event horizon has a different spatial topology in its early stages. At first sight

this is a bit confusing (it is also reminiscent of the changing spatial topology of the event horizon found recently in numerical simulations [12]). To see what goes on it is helpful to remember that space is really a torus with one asymptotic region. Then we can draw a faithful picture of the caustics at the bottom of the event horizon, and observe how the event horizon becomes smooth a moment after. See Figure 9, which then corresponds to a very particular slicing of our spacetime. After some reflection, one realizes that by changing the slicing a little bit a variety of spatial topologies for the event horizon can be obtained. This is however a slicing dependent statement of no particular importance.

Let us sketch the complications which occur in the general case. First the toroidal wormhole can be generalized by choosing a less symmetric fundamental region. This case is somewhat more difficult to analyze—a little care is needed to locate the event horizon. Nevertheless there are only very modest changes in the conclusions, and for this reason we do not give the details here. (The only noteworthy change is that the caustics no longer have to intersect in a single point.) For higher genus wormholes the situation is again very similar to the simple case that we have studied. The main conclusions are that it remains true in all cases that the domain of outer communication is isometric to the BTZ exterior (perhaps this is clearest in the “trousers” construction of the initial data), and that the black holes will be non-eternal since the event horizon is born at a time later than the birth of the universe in all cases.

To sum up the discussion so far, our black holes are not eternal. At early times the length of the event horizon is growing due to the presence of caustics. Indeed although the domain of outer communication is always isometric to the BTZ exterior (and hence static), the spacetime as a whole admits no global Killing vector at all. Nor does its exterior, which is larger than its domain of outer communication.

VI. Topological Censorship.

Our black hole can be described as the creation and collapse of a wormhole, or as a topological geon. A topological geon is a spacetime with a localized configuration having a non-Euclidean topology. Whenever there is a wormhole, a question concerning causality suggests itself: Is it perhaps possible to travel almost instantaneously through the wormhole between two points that are otherwise widely separated from each other? In four spacetime dimensions there are precise theorems that are relevant to this question. In particular it is known that an asymptotically flat spacetime with a non-simply connected Cauchy surface necessarily has a singular time evolution [13], so that the time available to send signals through a wormhole is limited. A very precise statement about this is the topological censorship theorem [1], which states that all causal curves connecting past and future null infinity are homotopic to a curve that lies in a simply connected neighborhood of null infinity. In this sense it is impossible to probe the interior topology actively from far away. Sufficient conditions for the

theorem to hold are asymptotic flatness, global hyperbolicity and the averaged null energy condition. A close relative of the theorem states that the domain of outer communication is simply connected. Note that the theorem does not entail the stronger notion of passive topological censorship, according to which the topology is unobservable from infinity. Indeed there are counterexamples to passive topological censorship.

Now the question is to which extent our wormhole agrees with these notions. Since our spacetime is asymptotically anti-de Sitter and not globally hyperbolic the answer is not quite obvious. Moreover \mathcal{F} has the topology of a cylinder and is not simply connected. Hence the domain of outer communication is not simply connected, not even for the BTZ black hole. On the other hand we know that the domain of outer communication is isometric to that of the BTZ black hole for all our examples, so that no further topological complications can be actively probed from infinity. In this sense, active topological censorship does hold for all our wormholes. A direct way to see what happens if one tries to send a signal from \mathcal{F} around the wormhole and back to \mathcal{F} is to choose a path that starts in one of the openings of the “tent” and ends at the opposite side. The minimum amount of sausage time required for such a trip is π , but we have seen that \mathcal{F} never lasts that long.

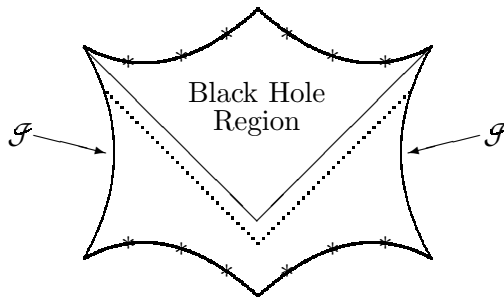


Fig. 10: A vertical slice through the stereographic image of the “tent”, centered on its center of symmetry. The solid light rays bordering the black hole region are the event horizon. The dotted lines are two light rays that reach \mathcal{F} in such a way that they violate passive topological censorship.

Nevertheless our black holes can be distinguished from the BTZ black hole, also from far away. To see how, choose a point on the “central line” going vertically through the fundamental region (i.e. on the line $\rho = 0$ if sausage coordinates are used) and to the past of the event horizon. Then connect it to \mathcal{F} by means of two light rays that end in different openings of the “tent”, which means that the light rays form a path that winds around the wormhole. (This is illustrated in Figure 10.) In other words we can see the full extent of the wormhole from infinity, even though we cannot travel through it. Therefore passive topological censorship does not hold for our wormholes.

VII. Apparent Horizons and Trapped Surfaces.

In this section we venture into the interior of our black holes in order to look for trapped curves. To define this notion, consider the two families of future directed null geodesics that are orthogonal to a closed curve in space. (If we were in 3+1 dimensions, we would have to define trapped surfaces instead, with appropriate changes in the definitions that follow.) If both families of light rays converge, there is clearly something non-trivial going on, and the curve is said to be trapped. It is an essential part of the definition that the curve be closed. The definition is important because there are singularity theorems that say that a singularity necessarily occurs to the future of an initial data surface that contains a trapped curve (although it may happen that the singularity is avoided if closed timelike curves appear [14]—a remark that is relevant to the spinning BTZ black hole). The theorems can also be proved under the assumption that an outer trapped curve occurs. An outer trapped curve (in a given spatial slice) is defined as the boundary of a two dimensional manifold-with-boundary whose outgoing light rays converge [15]. Note that a trapped curve need not be outer trapped since a trapped curve need not be the boundary of any region—trapped curves are allowed to intersect themselves, while outer trapped ones cannot do so. If the (outgoing) light rays have zero convergence the curve is said to be marginally (outer) trapped. Given a foliation of spacetime, a spatial region sitting inside an outer marginally trapped curve is called a trapped region, and the apparent horizon is ordinarily defined as the boundary of the union of all trapped regions. The conventional definition of the apparent horizon therefore demands that spacetime has been sliced into spatial hypersurfaces, it also depends strongly on this particular slicing (see eg reference [16] for a striking example). However, since our spacetimes are simple enough that we can find all the marginally trapped curves, we can afford to define the apparent horizon as the boundary of the spacetime region in which the trapped curves appear. Hence to us both the apparent horizon and the event horizon are spacetime concepts.

Let us consider the BTZ black hole first, because it is a particularly transparent case. To construct trapped curves in this case we just place vertices of two backward light cones anywhere on the line that represents the singularity. See Figure 11, where we employ stereographic coordinates so that lightcones appear as ordinary cones. The intersection of these light cones forms a flow line of the Killing vector J_{TY} that we use to identify points in anti-de Sitter space, and therefore it will be turned into a smooth closed curve by the identification. By construction both families of orthogonal light rays converge (namely to the vertices of the two light cones), and therefore this curve is trapped. Clearly there will be such a trapped curve through any point in the interior of the BTZ black hole. The event horizon is marginally trapped, since in that case the outgoing light rays lie on a null plane (with its vertex on the boundary of adS) and have zero convergence. In any spatial slicing the event horizon forms the

boundary of the trapped region, and therefore the apparent horizon coincides with the event horizon.

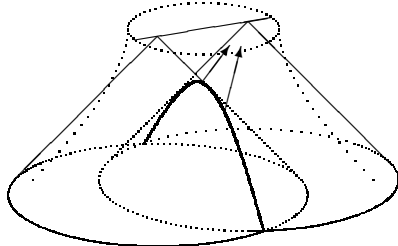


Fig. 11: Trapped curves in the BTZ black holes can be obtained as the intersection (heavily drawn hyperbola) of pairs of light cones whose vertices have been placed on the singularity. Since we use stereographic coordinates these light cones appear as ordinary cones in the picture. The outer, dotted hyperboloid represents infinity. The two converging arrows are lightlike normals on one side of the intersection; a similar pair exists on the other side, along the left light cone. This shows that the hyperbola is trapped.

Let us now consider the wormhole, and more particularly the simplest wormhole as defined in section V. The first observation is that any curve that lies in the event horizon and avoids the caustics is by construction marginally outer trapped, since the family of orthogonal outgoing light rays lies on the backwards light cone of the last point on \mathcal{S} . By deforming such a curve inward it is possible to find outer trapped curves in the interior. Therefore the main conclusion is again that the interior of the black hole is trapped, and that the apparent horizon coincides with the event horizon. (In 3+1 dimensions it is possible to construct a black hole which is locally isometric with anti-de Sitter space but for which this property does not hold [17].) A minor remark is that it is essential to require that the outer trapped curve bound a region: it is possible to find closed self intersecting curves for which one family of outgoing light rays converge and which extends beyond the event horizon. If such curves were admitted the theorem that the apparent horizon cannot lie outside the event horizon would not be true.

It is more interesting to look for curves that are trapped in both directions. Consider first the time symmetric initial data surface $U = 0$, and think of its covering space as a Poincaré disk. A geodesic will be closed provided that it meets the boundary of the disk at the fixed points of some transvection belonging to the isometry group which is used to identify points. Although the discrete isometry group has only two generators it has an infinite number of elements; indeed to every “word” in the generators a and b and their inverses there corresponds an element of Γ . Hence there are very many such fixed points, and indeed it is not difficult to convince oneself (by means of a tessellation of

the disk into copies of the fundamental region) that the closed geodesics fill the interior of the black hole densely, while there are none in the exterior.

We can also think of the initial data surface as a hyperboloid embedded in Minkowski space (compare Fig. 1a—stereographic projection is essentially an isometry for this surface). Then the geodesics are given by the intersection of the hyperboloid with some timelike plane through the origin; analytically

$$x_0X + y_0Y - \tau_0T = 0 \quad ; \quad x_0^2 + y_0^2 - \tau_0^2 = 1 . \quad (13)$$

But this is also the intersection of the initial data surface with two lightlike planes in adS, viz.

$$x_0X + y_0Y - \tau_0T \mp U = 0 . \quad (14)$$

Such a plane is the backwards light cone of a point on the boundary of adS having stereographic coordinates $\pm(x_0, y_0, \tau_0)$. Any such point on the boundary will have an image on the boundary of the fundamental region, at which the corresponding light rays in the black hole spacetime end. We can therefore conclude that any closed geodesic on the initial data surface is a marginally trapped curve in the black hole spacetime; the interior of the black hole in the initial data slice is densely covered with marginally trapped curves. Most but by no means all of them are self intersecting.

To the future of the marginally trapped curves genuinely trapped curves will appear. To see how this happens, consider an arbitrary closed geodesic in the initial data surface. By means of a global isometry of covering space it can be brought to coincide with a straight line through the center of the disk. It is a flow line of a unique transvection belonging to Γ and having a line of fixed points in anti-de Sitter space. This line coincides with the singularity of some BTZ spacetime (namely, the one whose group is generated by that unique transvection). Hence we can repeat the construction that gave us trapped curves there. Finally we undo the global isometry, and conclude that the trapped curve arises as the intersection of a pair of light cones suspended from a line of fixed points which (in stereographic coordinates) is precisely the straight line joining the points $-(x_0, y_0, \tau_0)$ and (x_0, y_0, τ_0) .

We have now constructed all marginally trapped curves. To see this it is enough to see that all families of light rays that have zero convergence have to converge to a point on \mathcal{S} . This is indeed so in $2 + 1$ dimensions where there can be no shear to complicate matters. To ensure that a spatial curve through such a null plane is closed it is necessary that its vertex lie on a fixed point of an element of the discrete isometry group that is used to identify points. But we have already accounted for the intersections of all such null planes. The generalization to more complicated wormhole spacetimes is straightforward and is omitted here.

VIII. Conclusions and Open Questions.

In this paper we have constructed all black holes which can be obtained by taking the quotient of a region of 2+1 dimensional anti-de Sitter space, which have one asymptotic region only, and whose fundamental group can be fully characterized by time symmetric initial data. Their event horizons and their trapped regions were displayed and it was shown in what sense topological censorship holds. The event horizons are not eternal, and have caustics which were described in some detail. Our account of the marginally trapped surfaces was complete. In general trapped surfaces are not so easy to find, so this clearly shows the advantages of working in 2+1 dimensions.

The restriction to one asymptotic region can easily be lifted (see ref. [2] for some possibilities in this direction). The restriction to time symmetric initial data on the other hand is less easily dispensed with. We accept a solution only if it has no naked singularities. For the time symmetric initial data we were able to analyze this requirement in detail, but we have been unable to make any progress in the general case. It is even conceivable that there are no further acceptable solutions. On the other hand, it may seem reasonable to expect that there should be a “spinning” wormhole as well. The BTZ black hole indeed admits a generalization with spin [4]. However, the nature of the singularities of this spacetime is quite different from that of the spinless BTZ black hole—in the spinning case there are no fixed point singularities, only (hidden) regions with closed timelike curves. As shown in ref. [17] a complete analysis of the causal structure in such situations is not straightforward. In particular the fundamental region—which was so useful in the case studied in the present paper—is no longer such a useful tool in the more general case. The spinning case is therefore open, and we have no final answer to the question of how many black holes with one asymptotic region there may be.

Another open question concerns quantum theory. We have nothing to say about this here, but we wish to stress that the motivation for studying black holes in 2+1 dimensions is not primarily to find instructive examples of the behavior of event horizons and the like—even though we have probably made it clear that we do find this interesting in itself. The primary motivation is that one may hope that 2+1 dimensional gravity can play the same role for quantum gravity that the Schwinger model played for QCD. We believe that the solutions described in this paper deserve study from this point of view.

Acknowledgement:

We thank Milagros Izquierdo for lessons in mathematics. IB and PP were supported by the NFR.

Appendix A

In the stereographic description—which was described more fully in ref. [5]—we project from one point in the embedded adS space to the tangent space T of the antipodal point. This tangent space inherits a flat, Lorentzian metric from the 4-dimensional embedding space. If we choose the center of projection at $(T, U, X, Y) = (0, -1, 0, 0)$ and the tangent space T at $U = 1$ with coordinates $x, y, \tau = X, Y, T$, this metric is simply

$$ds_{\text{flat}}^2 = -d\tau^2 + dx^2 + dy^2 . \quad (\text{A.1})$$

The projection of a point X^μ on the adS space (3) to a point x^μ in T is described by

$$x^\mu = \frac{2X^\mu}{U+1} \quad (X^\mu \neq U) , \quad (\text{A.2})$$

which defines another metric on T (corresponding to the adS geometry),

$$ds_{\text{adS}}^2 = \left(\frac{1}{1-r^2} \right)^2 (-d\tau^2 + dx^2 + dy^2) \quad \text{where} \quad r^2 = \frac{-\tau^2 + x^2 + y^2}{4} . \quad (\text{A.3})$$

Clearly the relation between the two metrics is *conformal*—as in the Euclidean context, stereographic projection is a conformal map.

This map does not cover all of adS space; we say that it is “centered on” the point antipodal to the center of projection (for the projection of Eq (16) the center is the point $(0, 1, 0, 0)$). Since a projection can be centered on any point, all of adS space can be covered by an atlas of such maps. The part of adS space which is covered by the stereographic projection is given by $U > -1$ and this region is mapped into the interior of a hyperboloid, $x^2 + y^2 - \tau^2 < 4$.

The isometries of adS space become certain conformal isometries of T that are in general not Lorentz transformations of the Minkowski metric; but those adS transformations that leave the origin of T fixed (and hence leave r constant) *are* also Lorentz transformations of the flat (inherited) metric of T . Thus any isometry of adS that has fixed points can be represented as a Lorentz transformation in a suitably centered stereographic projection. The projection centered on $(0, 1, 0, 0)$ is particularly suitable for our purposes since the Killing vectors that take the surface $U = 0$ into itself assume their familiar Minkowski space form (as generators of the three dimensional Lorentz group) in terms of the coordinates x, y and τ .

Appendix B

The sausage coordinates were fully described in earlier papers [6], so we can be brief. The idea is to introduce a time coordinate t such that

$$T = V \cos t \quad U = V \sin t . \quad (\text{B.1})$$

Then the equation for the anti-de Sitter hyperboloid and its metric become respectively

$$-V^2 + X^2 + Y^2 = -1 \quad (\text{B.2})$$

$$ds^2 = dX^2 + dY^2 - dV^2 - V^2 dt^2 . \quad (\text{B.3})$$

For constant t these are the equations that define the hyperbolic plane (embedded in Minkowski space). We arrive at the sausage coordinates t, ρ, ϕ if we introduce Poincaré's stereographic coordinates on the hyperbolic plane itself. The sausage coordinates are related to the embedding coordinates by

$$X = \frac{2\rho}{1-\rho^2} \cos \phi \quad Y = \frac{2\rho}{1-\rho^2} \sin \phi \quad (\text{B.4})$$

$$T = \frac{1+\rho^2}{1-\rho^2} \cos t \quad U = \frac{1+\rho^2}{1-\rho^2} \sin t . \quad (\text{B.5})$$

The metric in these coordinates is

$$ds^2 = - \left(\frac{1+\rho^2}{1-\rho^2} \right)^2 dt^2 + \frac{4}{(1-\rho^2)^2} (d\rho^2 + \rho^2 d\phi^2) . \quad (\text{B.6})$$

A useful fact is that it takes an amount of sausage time $t = \pi/2$ for a light ray to go from the origin to \mathcal{F} . A word of warning concerns pictures such as our Figure 8. The point is that the Killing vectors that we use to generate the identifying isometries do not lie in the disks of constant t , except for the particular disk at $t = 0$. In Figure 8, disks at different t values are shown, and it may appear as if the event horizon has kinks at the boundaries of the fundamental region. This is not so; the event horizon is indeed smooth, but the disks are not (except when $t = 0$).

References

- [1] J.L. Friedman, K. Schleich and D.M. Witt, Phys. Rev. Lett. 71 (1993) 1486.
- [2] D. Brill, Phys. Rev. D53 (1996) R4133.
- [3] A. Steif, Phys. Rev. D53 (1996) 5527.
- [4] M. Bañados, C. Teitelboim and J. Zanelli, Phys. Rev. Lett. 69 (1992) 1849.
M. Bañados, M. Henneaux, C. Teitelboim and J. Zanelli, Phys. Rev. D48 (1993) 1506.
- [5] D. Brill, Geometry of Black Holes and Multi-Black-Holes in 2+1 Dimensions, in P. Joshi (ed): Singularities, Black Holes and Cosmic Censorship, Inter-University Centre for Astronomy and Astrophysics 1996, ISBN 81-900378-2-X, gr-qc/9607026.
- [6] S. Holst, Gen. Rel. Grav. 28 (1996) 387.
S. Åminneborg, I. Bengtsson, S. Holst and P. Peldán, Class. Quant. Grav. 13 (1996) 2707.
- [7] C.W. Misner, in J. Ehlers (ed.): Relativity Theory and Astrophysics, American Mathematical Society, Providence RI 1967.
- [8] R. Benedetti and C. Petronio, Lectures on Hyperbolic Geometry, Springer 1992.
- [9] S. Deser, R. Jackiw and G. 'tHooft, Ann. Phys. 152 (1984) 220.
- [10] G. Mess, Lorentz Spacetimes of Constant Curvature, IHES preprint, April 1990.
- [11] A. E. Fischer, The Theory of Superspace in Carmeli, Fickler and Witten (eds): Relativity, Plenum 1970; Gen. Rel. Grav. 15 (1983) 1191.
Chapter 43 in C.W. Misner, K.S. Thorne and J.A. Wheeler, Gravitation, W. H. Freeman and Co. 1973.
- [12] S.L. Shapiro, S.A. Teukolsky and J. Winicour, Phys. Rev. D52 (1995) 6982.
- [13] D. Gannon, J. Math. Phys. 16 (1975) 2364.
- [14] R.P.A.C. Newman, Gen. Rel. Grav. 21 (1989) 981.
- [15] R.M. Wald, General Relativity, University of Chicago Press, Chicago 1984.
- [16] R.M. Wald and V. Iyer, Phys. Rev. D 44 (1991) R3719.
- [17] S. Holst and P. Peldán, Black Holes and Causal Structure in Anti-de Sitter Isometric Spacetimes, gr-qc/9705067.